Fluid Mechanics
2020; 6(1): 15-29
http://www.sciencepublishinggroup.com/j/fm
doi: 10.11648/j.fm.20200601.12
ISSN: 2575-1808 (Print); ISSN: 2575-1816 (Online)

Quinn's Law of Fluid Dynamics: Supplement #2 Reinventing the Ergun Equation

Hubert Michael Quinn

Department of Research and Development, the Wrangler Group LLC, Brighton, USA

Email address:
hubert@wranglergroup.com

To cite this article:
Hubert Michael Quinn. Quinn's Law of Fluid Dynamics: Supplement #2 Reinventing the Ergun Equation. *Fluid Mechanics*. Vol. 6, No. 1, 2020, pp. 15-29. doi: 10.11648/j.fm.20200601.12

Received: March 17, 2020; **Accepted**: May 13, 2020; **Published**: June 15, 2020

Abstract: This paper is directed at the important contribution to fluid dynamics made by Sebri Ergun. In his three papers published in 1949, 1951 and 1952, using various gases as his percolating fluid, Ergun used his empirical permeability results of packing conduits with fractured coke (irregularly shaped particles), in combination with some theoretical concepts, to generate an equation which captured the viscous and kinetic contributions to packed conduit permeability in two separate terms in that equation, resulting in his now famous "Ergun Equation". In addition, he identified a discrete "constant" for each of the terms which we label herein the "viscous" and "kinetic" constants, respectively. We demonstrate herein, however, that the values assigned by Ergun to both his constants are not certifiable and, thus, are problematic in predicting the permeability of packed conduits. Moreover, since the publication of his 1952 paper, in which he disclosed the values of 150 and 1.75 for the viscous and kinetic constants, respectively, many scholarly works have been published which claim to validate these values. As a result, these values have become erroneously embedded in conventional folklore concerning fluid flow in closed conduits and have enjoyed widespread acceptance as being a legitimate feature of fluid dynamics dogma. With the advent recently of Quinn's Law, a novel approach to the understanding of fluid flow in closed conduits, we are able to articulate in a manner not heretofore possible, the significance of this discrepancy in Ergun's values of the constants, which we demonstrate is far too important to ignore.

Keywords: Viscous Constant, Kinetic Constant, Ergun Equation, Friction Factor, Transition Region, Turbulent Flow, Wall Effect, Boundary Layer

1. Introduction

We begin by defining the problem in light of the recent publication of Quinn's Law which, for the first time, provides a comprehensive analytical road map for the comparison of packed conduit permeability both in the laminar and turbulent regions of the fluid flow regime. This is a critical feature of Quinn's Law, since the Ergun equation is supposed to be accurate over the entire range of the fluid flow regime, because one can now use the permeability of an empty conduit as an independent reference point against which one can titrate the permeability results for packed conduits across the entire spectrum of the fluid flow regime. Furthermore, we will establish the magnitude of the problem posed by the erroneous values of the constants in Ergun's equation, by showing a comparison between the dictates of Quinn's Law for a typical packed conduit in routine use today for HPLC (High Pressure Liquid Chromatography) analyses [1], and the Ergun equation, both in the laminar (linear) and turbulent (non-linear) regions of the fluid flow regime [2-4].

Let us consider, therefore, a worked example in which a conduit packed with spherical rigid particles to an external porosity of 0.40 (a measure of its packing density). This is a typical packed conduit in use today in major pharmaceutical companies for the analysis of routine samples in the drug discovery market segment. Let us assume also that we are pumping water through the packed conduit at such a rate that we cover a range of modified Reynolds number values between 0.1 (laminar) and 120,000 (turbulent). We show this scenario in Figure 1.

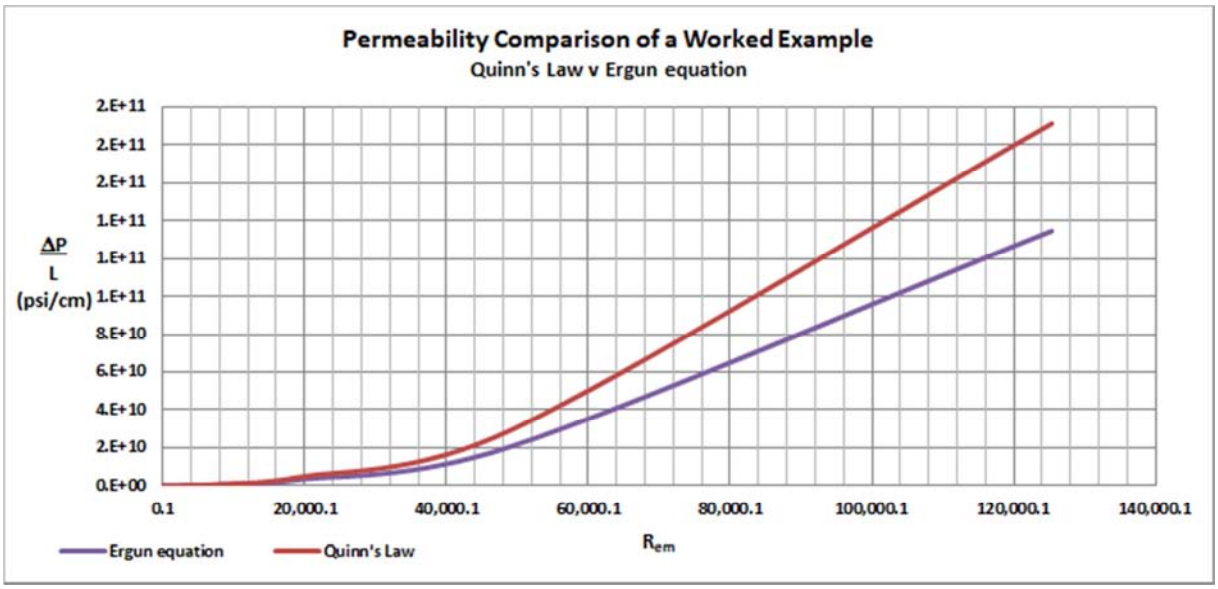

Figure 1. *Permeability Comparison.*

As shown in Figure 1, we have captured the permeability profile for this worked example based upon the dictates of both the Ergun equation and Quinn's Law, showing the pressure gradient in units of psi/cm on the y-axis and the dimensionless modified Reynolds number on the x-axis. It is obvious from the plot that the Ergun equation understates the pressure drop across the conduit as compared to Quinn's Law. Moreover, the discrepancy between the two models becomes significantly greater with higher values of the modified Reynolds number. Indeed, we can see that the difference in the total pressure drop varies from 600 psi (approx.) at the lowest value of the Reynolds number (0.1), to 60,000,000 psi (approx.) at the highest value of the modified Reynolds number. Thus, it is not an overstatement to assert that, if validated, this discrepancy is too important to ignore.

We may now pose the question; which fluid flow model is to be believed and what are the fundamental differences between the two? To answer this question we turn to the empirical evidence.

2. Methods

We have chosen a very specialized experimental setup to carry out the validation of Quinn's Law *vis-a-vis* the Ergun equation for packed conduits. It will become increasingly apparent below why the experimental methodology is so specialized and why, in particular, we have avoided the usual experimental methodology, which invariably is the root cause of the erroneous assertions regarding the value of the constants found throughout the literature of packed conduit permeability.

2.1. Experimental Setup

Our experimental apparatus was assembled as a prototype instrument designed for doing continuous flow chemistry. It consists of a fluid flow loop with calibrated pressure transducers for measuring pressure drop; several rtds along the pipe flow loop to monitor temperature at different locations; a circular gear pump to provide fluid flow up to a maximum of 200 psi; a computerized control system running LabView software manufactured by National Instruments. Large plastic reservoirs were filled with water at room temperature and the water was continuously recycled throughout the experiments. Graduated cylinders were used in conjunction with the stop watch in the computer to accurately measure the fluid flow rate. The voltage of the power supply controlling the gear pump was set in the software, and for each flow rate measurement, the temperature and pressure drop across the packed conduit was recorded.

The packed conduit used in these experiments is very unique and designed especially for the purpose of this publication study. It consists of a conduit made of PFA plastic into which totally spherical stainless steel electro-polished ball bearings were packed. The ball bearings were each placed one-by-one into the conduit by hand. The diameter of the ball bearings was 0.329 cm and the diameter of the conduit was 0.368 cm. A total of four different conduit nominal lengths were packed, 20, 40, 60 and 100 cm, and their permeability measured. For each packed conduit, the number of stainless steel ball bearings was counted and the column length was defined accordingly i.e., the plastic conduit was cut off at this corresponding length of bed height. Consequently, the length of the packed conduit was validated by the number of particles packed therein, which was always an exact integer, i.e., no partial particles.

Thus, because the particle diameter was just slightly less than the conduit diameter, each particle sat on top of one other and the column length was therefore equivalent to the total number of particles multiplied by the average spherical diameter equivalent of an individual particle. The size distribution of the particle diameters at this magnitude of

value was extremely low, as documented by caliper measurements and, therefore, the average particle diameter, d_p, and the number of particles packed into the conduit, n_p, were calibrated against one another. Accordingly, the exact column lengths were; 56 × 0.329=18.43 cm; 114 × 0.329=37.52 cm; 173 × 0.329=56.94 cm; 297 × 0.329=97.75 cm, which corresponds to packed conduits containing, 56, 114, 173, and 297 individual steel ball bearings, respectively.

This methodology of preparing the packed conduits for this study is critical because it eliminates any potential error in the values of the combination of average spherical particle diameter equivalent, d_p, packed conduit external porosity (packing density), ε_0, and the number of particles, n_p, packed into the conduit under study. Furthermore, it guarantees that the external porosity is identical in each of the four packed conduits in this study. Thus, the value of the external porosity was ε_0=0.467 for these experiments. This experimental protocol is important because, as we shall demonstrate below, this combination of values is critical in establishing a correlation between measured and calculated values, especially in the nonlinear portion of the fluid flow regime, when using theoretical fluid flow models and measured permeability based upon measured variables for packed conduits.

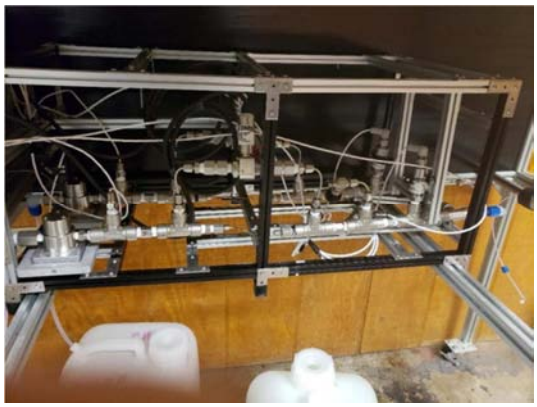

Figure 2. *Photograph of fluidics module.*

The particles were retained in the packed conduits by coarse retaining stainless steel screens at both ends. We were careful to measure the pressure drop across these retaining screens and subtract it from the total measured pressure drop for each conduit. In addition, the use of four different packed conduit lengths validates the contribution of the end-fitting screens.

We show three photographs of the experimental set up; Figure 2 is the fluidics module; Figure 3 is the packed conduit used; Figure 4 is the electronics module and computer control unit.

Figure 3. *Photograph of Packed Conduit.*

Figure 4. *Photograph of Electronics and computer control module.*

A total of approximately 100 separate measurements were taken and the results are tabulated in Table 1.

Table 1. *Measured Results.*

Voltage		Q	Temp	ΔP		Q	Temp	ΔP
				Actual				Actual
volts		ml/min	°C	psi		ml/min	°C	psi
0.40	**60 cm**	**66**	**19**	**3**	**40 cm**	**36**	**19**	**1**
0.50		80	19	4		46	19	1
0.60		98	19	6		57	19	1
0.70		115	19	8		65	19	2
0.80		130	19	9		77	19	2
0.90		145	19	12		88	19	3
1.00		160	19	14		97	19	4
1.10		175	19	17		107	19	4
1.20		190	19	19		120	19	5
1.30		205	19	23		130	19	6
1.40		220	19	26		145	19	8
1.50		235	19	29		158	19	9

Voltage		Q	Temp	ΔP		Q	Temp	ΔP
				Actual				Actual
volts		ml/min	°C	psi		ml/min	°C	psi
0.40	**60 cm**	**66**	**19**	**3**	**40 cm**	**36**	**19**	**1**
1.60		250	19	33		174	19	11
1.70		265	19	37		183	19	12
1.80		275	19	40		200	19	14
1.90		290	19	44		215	19	16
2.00		305	19	49		225	19	18
2.10		320	19	53		238	19	20
2.20		335	19	58		255	19	23
2.30		350	19	64		270	19	25
2.40		360	19	67		280	19	27
2.50		375	19	73		300	19	31
2.60		387	19	77		306	19	32
2.70		405	19	84		325	19	36
2.80		420	19	91		335	19	38
2.90		430	19	95		350	19	42
3.00		437	19	98		360	19	44

Table 1. *Continued.*

Voltage		Q	Temp	ΔP		Q	Temp	ΔP
				Actual				Actual
volts		ml/min	°C	psi		ml/min	°C	psi
0.40	**20 cm**	**52**	**19**	**1**	**100 cm**	**55**	**19**	**3**
0.50		65	19	1		69	19	5
0.60		78	19	1		83	19	7
0.70		92	19	2		96	19	9
0.80		105	19	2		109	19	12
0.90		116	19	2		125	19	15
1.00		125	19	3		136	19	18
1.10		135	19	3		150	19	21
1.20		150	19	4		163	19	25
1.30		163	19	5		175	19	29
1.40		175	19	5		188	19	33
1.50		191	19	6		200	19	45
1.60		210	19	8		212	19	41
1.70		235	19	9		225	19	46
1.80		250	19	11		238	19	52
1.90		270	19	12		250	19	57
2.00		290	19	14		265	19	63
2.10		305	19	16		280	19	71
2.20		315	19	17		293	19	77
2.30		330	19	18		303	19	82
2.40		352	19	21		315	19	89
2.50		365	19	22		325	19	94
2.60		380	19	24		340	19	103
2.70		397	19	26		350	19	109
2.80		410	19	28		370	19	122
2.90		420	19	29		375	19	125
3.00		435	19	31		385	19	131

2.2. Experimental Results

As shown in Figure 5, we have captured our measured results for the packed conduits containing the stainless ball bearings using four different lengths, to which we have given the reference number HMQ-14, and plotted them as pressure gradient, ΔP/L, in units of psi/cm versus fluid flow rate, Q, in units of mL/min. We have shown on the plot for comparison purposes, the data of Farkas et al [5] and the data from our previous paper for empty conduits [6]. As can be seen from the plot, our flow rates varied between a low value of 30 mL/min and a high value of 500 mL/min. The corresponding range of total pressure drops measured was from a low of 0.5 to a high of 135psi.

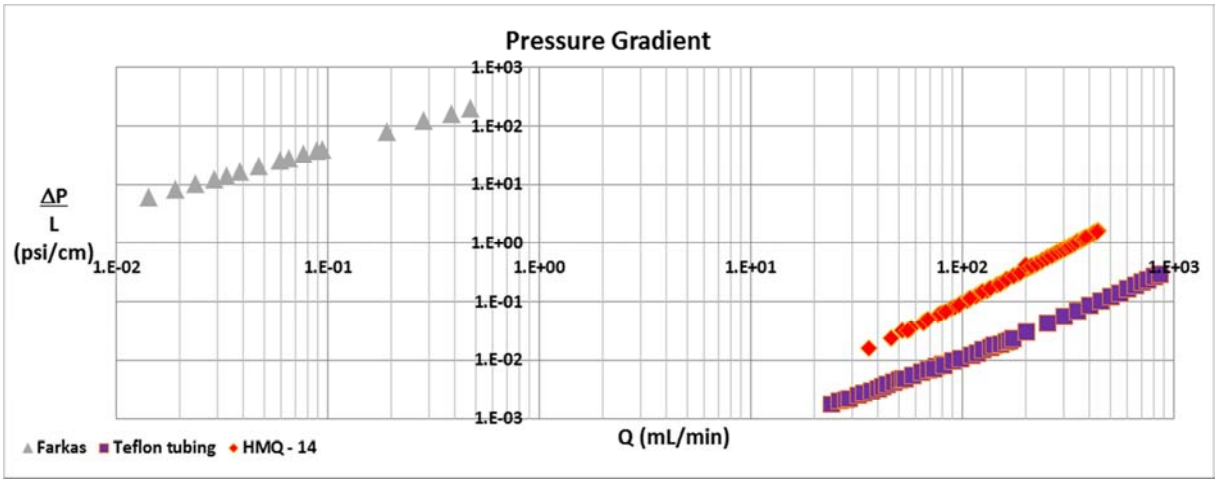

Figure 5. *Measured Results Comparison.*

We will now refer to the Quinn Fluid Flow Model (QFFM) [1] to establish a correlation between our measured data and that implicit in Quinn's Law.

We begin with equation (63) found in the original publication for Quinn's Law [1]. This is the equation that relates the pressure gradient to other conduit parameters;

$$\frac{\nabla P}{L} = \frac{4\pi {r_h}^3 n_v}{3} + \frac{\delta \lambda n_k}{2\pi} \tag{1}$$

Where, ΔP/L=the pressure gradient; r_h=the normalization coefficient of fluid drag=4; δ porosity coefficient; λ=the fluid current wall-effect normalization coefficient; n_v=the viscous force per unit volume; n_k=the kinetic force per unit volume.

Substituting for r_h in equation (1) gives;

$$\frac{\Delta P}{L} = \frac{4\pi 64 n_v}{3} + \frac{\delta \lambda n_k}{2\pi} \tag{2}$$

Simplifying equation (2) gives;

$$\frac{\Delta P}{4L} = 67 n_v + \frac{\delta \lambda n_k}{8\pi} \tag{3}$$

We can see from equation (3) that the pressure gradient term on the left hand side of equation (3) is the sum of a viscous and a kinetic term, both of which appear on the right hand side of equation (3). Normalizing for the viscous contributions, we divide across equation (3) by the term n_v. Thus we get;

$$\frac{\Delta P}{4Ln_v} = 67 + \frac{\delta \lambda R_{em}}{8\pi} \tag{4}$$

Where $R_{em}=n_k/n_v$

Rearranging equation (4) we get;

$$\frac{\Delta P}{4Ln_v} = 67 + \frac{\lambda Q_N}{8\pi} \tag{5}$$

Where $Q_N=\delta R_{em}$.

Rearranging equation (5) we get;

$$P_Q = 67 + \frac{C_Q}{8\pi} \tag{6}$$

Where $C_Q=\delta Q_N$.

Finally, equation (6) may be written as;

$$P_Q = k_1 + k_2 C_Q \tag{7}$$

Where $k_1=64\ \pi\ /3=67$ (approx.) and $k_2=1/8\ \pi=0.04$ (approx.)

Equation (7) is known as Quinn's Law of fluid dynamics.

We can see then that the term P_Q in the QFFM is a viscous type friction factor because it represents the measured pressure drop, normalized for viscous contributions, and is a linear function of the term C_Q over the entire range of the modified Reynolds number which is an embedded term in C_Q.

In Figure 6 we show a plot of our measured results as a function of the modified Reynolds number as well as our calculated values based on the QFFM. Note the excellent correlation between the measured and calculated values. As can be seen in the plot, the flow rates used in the experiments correspond to a range of modified Reynolds number values from 300 to 4,000 and includes all three regions of the flow regime, i.e., laminar, transition and turbulent.

Next we present our measured results in the dimensionless form of Quinn's Law, i.e., after equation (6).

In Figure 7 we show a plot of our measured results in the dimensionless parameters taught in the QFFM namely, viscous friction factor P_Q, versus wall-effect normalized fluid current C_Q. The plot is log-log and covers a range of Reynolds number values from 1×10^{-4} to 1×10^{7} which represents a range of 11 orders of magnitude. The plot describes a straight line of slope $1/8\ \pi=0.04$ approximately, and intercept on the y-axis of $64\ \pi\ /3=67$ approximately. As a means of validating our measured results, we also show on the plot the third party published results of Farkas [5] and the line for λ=1 which represents all typical packed conduits [1].

We include the packed conduit data from the paper by Farkas et al because it enables us to validate the curve at extremely low values of the modified Reynolds number, i.e., creeping flow.

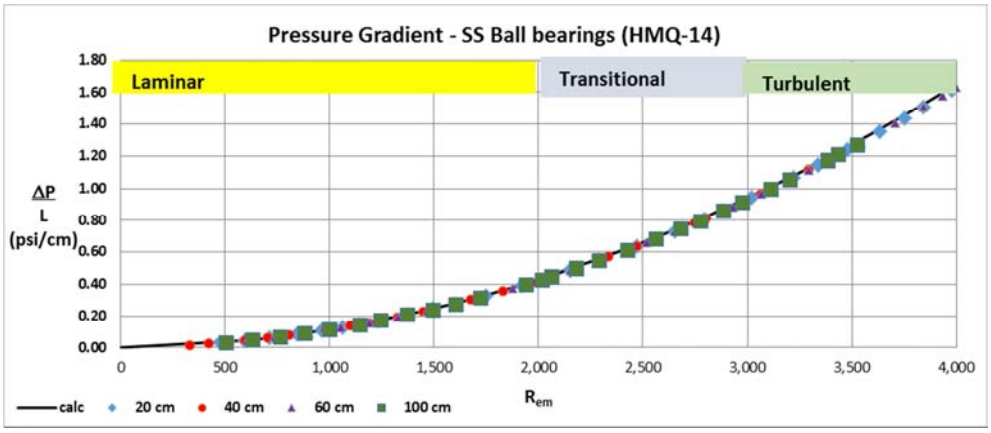

Figure 6. *Empirical Data Dimensional.*

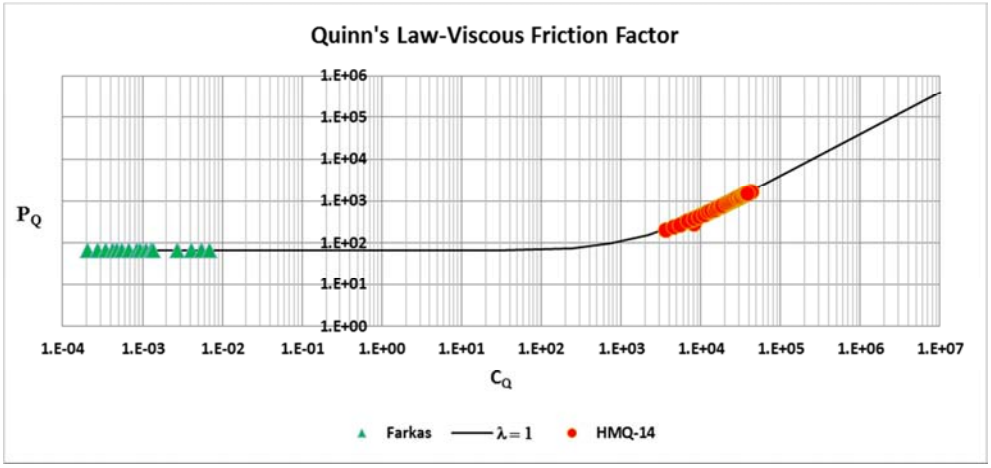

Figure 7. *Empirical Data Dimensionless.*

3. Modeling Our Results After Ergun

Next we present our measured results in the format of Ergun's equation. In order to accomplish this task we must express Quinn's law in the format of the Ergun equation.

We begin with Quinn's Law from equation (7) above:

$$P_Q=k_1 + k_2C_Q$$

Multiplying equation (7) across by r_h, we get:

$$r_hP_Q=k_1r_h + r_hk_2C_Q \quad (8)$$

Substituting for C_Q in equation (8), we get:

$$r_hP_Q=k_1r_h + r_hk_2\delta\lambda R_{em} \quad (9)$$

Reformatting equation (9), we get;

$$f_v=A + BR_{em} \quad (10)$$

Where, $f_v=r_hP_Q$, $A=k_1r_h$, $B=r_hk_2\delta\lambda$

Substituting for r_h in equation (10), we get:

$$f_v=4P_Q \quad (11)$$

$$A=268.19 \quad (12)$$

$$B=\frac{\delta\lambda}{2\pi} \quad (13)$$

Equation (10) represents Quinn's Law expressed in the general format of the Ergun equation, which we will refer to henceforth as the Q-Modified Ergun equation.

We can see then that the difference between Quinn's Law and the Ergun equation can be distilled down to two parameters,

1. The value of the viscous constant A=268 (approx.), in Quinn's law, whereas it has the value of 150 in the Ergun equation.
2. The value of the kinetic constant $B=\delta/2\pi$ ($\lambda=1$ for packed conduits) in Quinn's Law, whereas it has the constant value of 1.75 in the Ergun equation.
3. As shown in Figure 8, we have plotted the experimental results for 10 micron silica particles reported in the Farkas paper after the Q-modified Ergun equation (10). Note that in this straight line plot the intercept represents the value of A and the slope the value of B. Note that the value of A is validated at 268 (approx.) and the value of B at 2.47 (approx.). Thus we can see that this third party empirical data differs from the Ergun values of 150 and 1.75 for the viscous and kinetic constants, respectively.
4. Next we will evaluate our measured results in this same Ergun format.

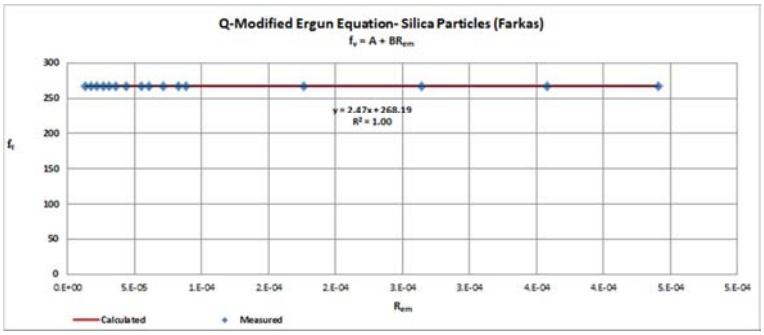

Figure 8. *Silica Particles.*

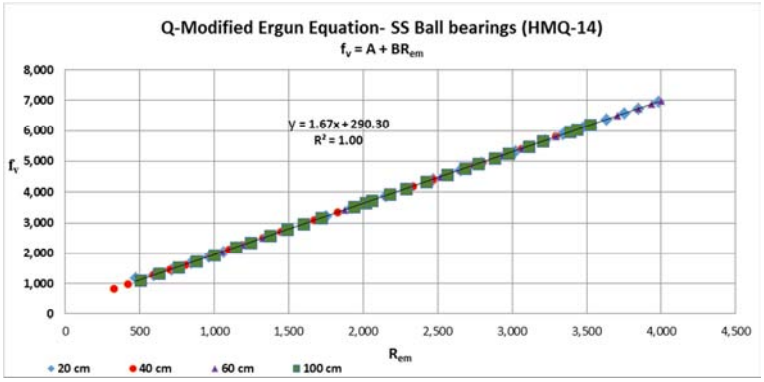

Figure 9. *SS Ball Bearings.*

In our Figure 9, we have plotted the results of our stainless steel ball bearing packed conduits (HMQ-14). We note that all four packed conduits fall on the same straight line with intercept 290 and slope 1.67. Since we did not measure sufficient data points at a low enough value of the modified Reynolds number, the value for A is slightly elevated, i.e., 290.

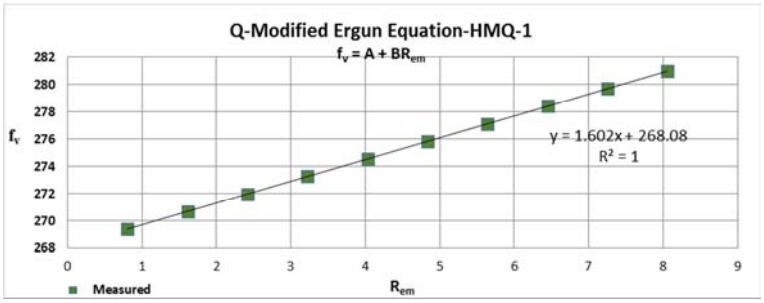

Figure 10. *Polymeric Particles.*

In our Figure 10, we have plotted the results of our rigid polymeric particle packed conduit (HMQ-1) reported elsewhere (Quinn 2019). This data set demonstrates values for A of 268 (approx.) and B of 1.60, respectively.

4. The Significance of Ergun's Erroneous Values for the Constants

We can now understand better the problem presented by Ergun's erroneous values for both constants, A and B (Quinn 2014, Giddings 1965).

On the one hand, his equation understates the true values in the laminar region of the flow regime because his value of 150 for the viscous constant is too low. On the other hand, his equation does not correctly represent the true pressure gradient in the turbulent regime for two reasons; (1) Ergun's value of 1.75 for B is a constant but, (2) the true value of B is not constant. Rather, it is a function of the term δ in Quinn's Law which, in turn, is a function of the external porosity of the packed conduit under study, ε_0. Thus, based upon the teaching of Quinn's law, we may write:

$$B = \frac{\delta}{2\pi} = \frac{1}{2\pi\varepsilon_0{}^3} \tag{14}$$

Accordingly, for measured data in the turbulent regime, Ergun's equation may understate or overstate the true pressure gradient, depending upon the external porosity of the packed conduit. Additionally, and to make matters even more confusing, depending again upon the combination of the external porosity of the packed conduit under study and the modified Reynolds number range, it may correctly state the pressure gradient pursuant to a phenomenon similar to

that of a "stopped watch" which, as we all know, correctly states the time twice per day. We can illustrate this best as in Figure 11.

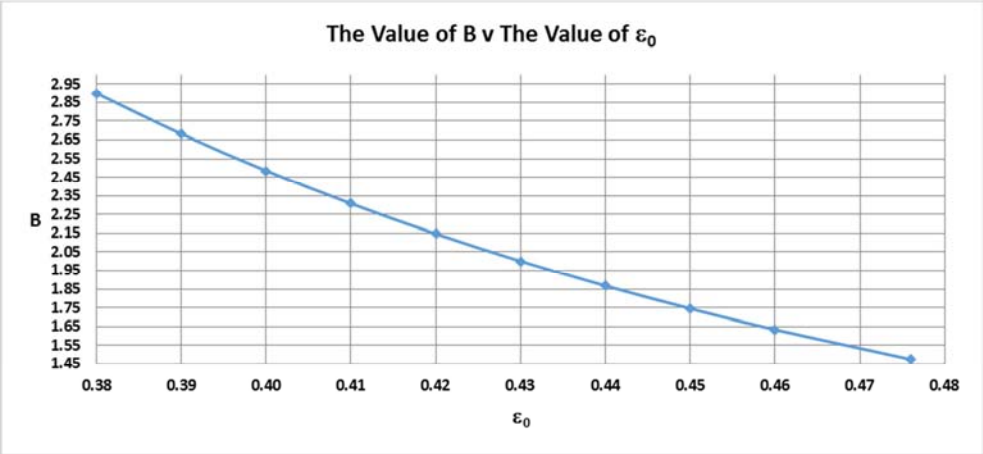

Figure 11. *Q-Modified Value of B.*

In our Figure 11 we show a plot of the value of B against the value of ε_0. Accordingly, we can make the following conclusions concerning the characteristics of the Ergun equation:

1. The Ergun equation will always understate the pressure gradient when measurements are made in the laminar flow regime. This is because Ergun's value of 150 for A is less than the true value of A which is always 268 (approx.) and the kinetic term of the equation is virtually neglect able.
2. The true value of B is greater than 1.75 for all packed conduits having a value of ε_0 less than 0.45. Thus, in this scenario, the Ergun equation will understate the true pressure gradient for all values of the Reynolds.
3. The true value of B is equal to 1.75 for all packed conduits having a value of ε_0 equal to 0.45. Thus, in this scenario, the Ergun equation will tend to correctly represent the pressure gradient as the values of the modified Reynolds number tend upwards into the fully turbulent regime.
4. The true value of B is less than 1.75 for all packed conduits having a value of ε_0 greater than 0.45. Thus, in this scenario, the Ergun equation will overstate the pressure gradient as values of the modified Reynolds number tend upwards into the turbulent regime.

To highlight the above conclusions, we turn, once again, to our experimental evidence.

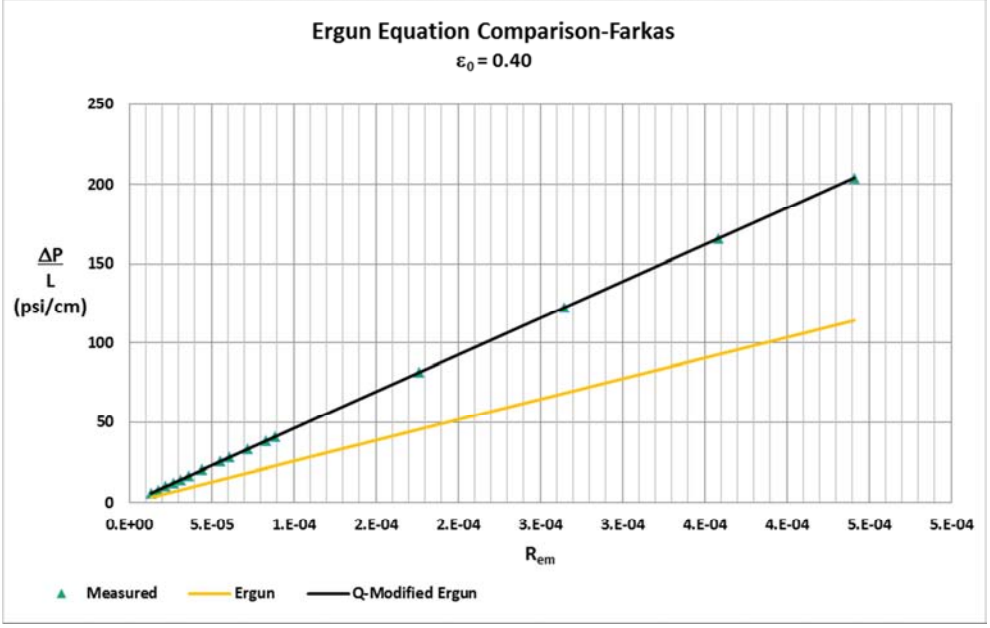

Figure 12. *Comparison of Ergun Equations-Silica Particles.*

As shown in Figure 12, the Ergun equation understates the pressure gradient for the data reported in the Farkas et al paper. This is due to the very low values of the modified Reynolds numbers for the data set, i.e. creeping flow. On the

other hand, the Q-modified Ergun equation correctly captures the measured values.

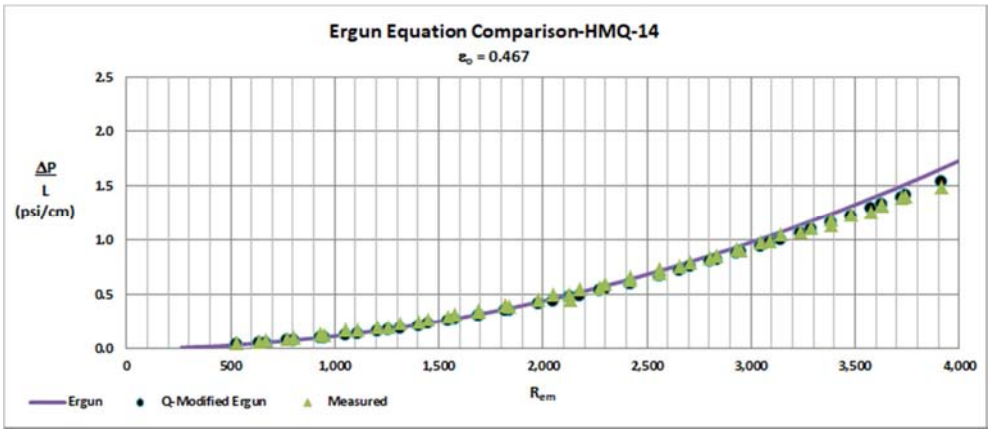

Figure 13. *Comparison of Ergun Equations –SS Ball bearings.*

As shown in Figure 13, the Ergun equation and the Q-modified Ergun equation show an increasing discrepancy at higher values of the modified Reynolds number. This is because, (a) the value of the external porosity for the HMQ-14 packed conduits, all have a value of 0.467, and, (b) the measured values are all taken at relatively high values of the modified Reynolds number.

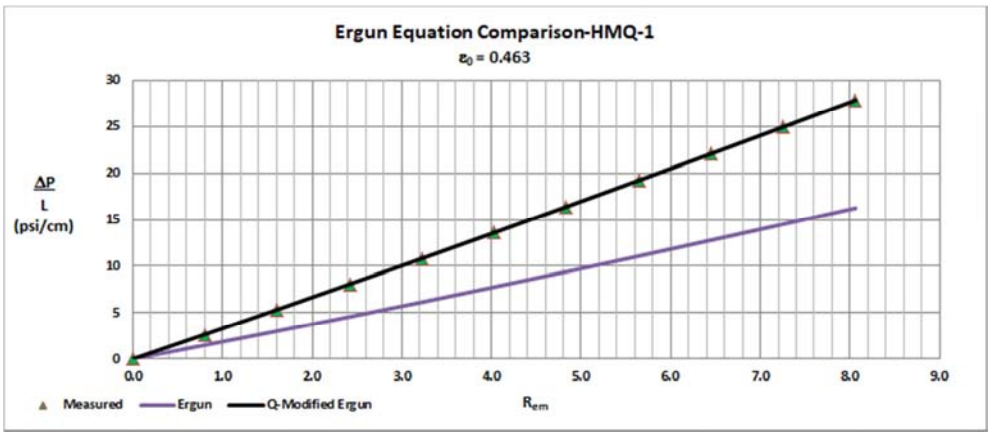

Figure 14. *Comparison of Ergun Equations-Polymeric Particles.*

In our Figure 14, we demonstrate that the Ergun equation understates the pressure gradient for the measured data reported in the packed conduit identified as HMQ-1. This is because this measured data set was for a packed conduit having a value of ε_0=0.463 and the measurements were taken at relatively moderate modified Reynolds number values [7]. As is also apparent in the plot, the Q-modified Ergun equation correctly captures the measured data.

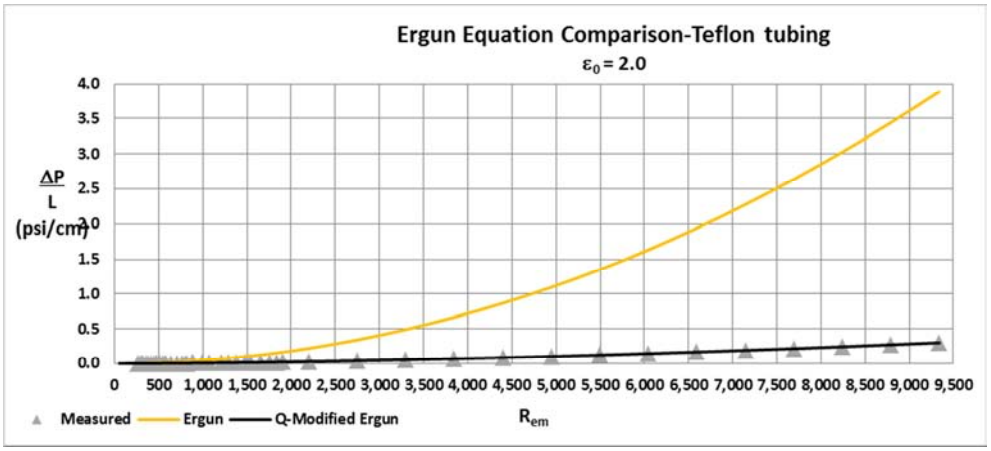

Figure 15. *Comparison of Ergun Equations-Empty Conduit.*

In our Figure 15, we demonstrate that the Ergun equation grossly overstates the pressure gradient for the measured empty conduit data reported in our previous paper [6]. We make this assertion based upon the unique feature of Quinn's Law which allows a comparison between the permeability of an empty and packed conduit [8]. Thus, we see that the error created by the values of Ergun's constants can be enormous when there is a large value of ε_0. Again, the Q-modified Ergun equation correctly captures the measured data.

5. Our Experimental Methodology Explained

We have stated above that our experimental methodology disclosed herein is unique in the literature of packed conduit permeability. We now focus on the reasons underlying this assertion.

Once again, we refer to the original publication of Quinn's Law [1] (using the same equation numbers therein) to identify the critical relationships between variables pertaining to this aspect of our methodology.

Firstly, we can see from equation (21) therein, that the conduit external porosity is a function of four independent variables:

$$\varepsilon_0 = 1 - \frac{2n_p {d_p}^3}{3d^2L}$$

Where, ε_0=the packed conduit external porosity, n_p is the number of particles of diameter d_p contained in the packed conduit, d_p is the average spherical particle diameter equivalent of the particles packed in the conduit, D is the diameter of the conduit and L is the length of the conduit.

Moreover, it is obvious from equation (21) also that for a fixed value of external porosity, ε_0, every discrete value of d_p must have a matching value for n_p, in any given conduit under study. In our experimental methodology for establishing the value of the external porosity, ε_0, we have measured independently all 4 independent variables in equation (21) and, therefore, this relationship was vigorously adhered to, but in virtually every other experimental methodology found in the literature, this is not the case. The principle defined by this relationship, in turn, is a dictate of continuity embedded in the Laws of Nature.

Secondly, we can see from equation (38) therein, that the normalization coefficient of fluid drag is especially important:

$$r_h = \frac{SA_P}{CSA_P} = 4$$

Where, SA_p=the surface area of a spherical particle and CSA_p=the cross sectional area of a spherical particle.

Thus, as shown in equation (38) also, the value of r_h is, not only, constant, but also, it is independent of particle diameter. This fact dictates that the value of 268 (approximately) in the Q-modified Ergun equation is also a constant.

5.1. A worked Example from the Literature

In order to underscore the importance of our experimental protocol disclosed herein and to distinguish it from that used generally in the literature, we now focus on a worked example from a recent publication in the literature of a well-known author of packed conduits, J. H. Van Lopik et al [9, 10]. In both these papers, the authors are focused on the nonlinear flow behavior in packed conduits. In other words, they are investigating the relationship between mixtures of blended particles in packed conduits and measured pressure drop versus flow rate, when that pressure drop is related to the fluid flow velocity in a nonlinear fashion. In the 2017 paper, the authors studied the effect of grain (particle) size distribution on the nonlinear flow behavior in sandy porous media using well-characterized reference particles. In the 2019 paper, on the other hand, they used samples of particles which were both more irregular in shape and more varied in diameter than the 2017 study, thus producing packed conduits which were more diverse in their flow characteristics.

5.1.1. Foreword

Before we get into the details of the worked example, and to help the reader get a grasp of where we are going in this exercise, we need to state upfront a dictate of nature concerning nonlinear flow behavior in packed conduits, which has only been brought to light recently by the teaching of Quinn's Law. That dictate is that there exists within the natural world only one combination of average spherical particle diameter equivalent, d_Q, packed conduit external porosity, ε_0, modified Ergun coefficient values of A and B, that will correlate permeability flow behavior over the entire range of the fluid flow regime. The authors have adopted, in both papers of this worked example, the Forchheimer relationship, which identifies the characteristic relationship between pressure drop, ΔP, in our terminology, and fluid flow velocity, μ_s, in our terminology. They rightly point out that this relationship is quadratic (2^{nd} power) in the kinetic term and linear (1^{st} power) in the viscous term with respect to fluid velocity and, accordingly, defines the unique Forchheimer correlation coefficient values of, a, and, b. As will become clearer below, however, we will demonstrate that in both papers of this worked example, the reported values for the modified Ergun coefficients, A and B, do not correlate the measured data.

5.1.2. Our Analysis

In the abstract of the 2017 paper, the authors recite that "numerical and experimental studies show that the flow resistance in porous media is largely determined by geometry of the pore structure". As demonstrated above, we know that, regarding permeability in packed conduits, continuity dictates that every discrete value of particle diameter, d_p, assigned to a particular packed conduit under study, must be accompanied by a correspondingly matched value of external

porosity, ε_0, in addition to the number of particles present, n_p, since it is this combination of packed conduit parameters that, (a) guarantees that all free space in the packed conduit is properly accounted for and, (b) precisely determines the "geometry of the pore structure". However, in this 2017 paper, the author's experimental protocol does not recognize this dictate of the Laws of Nature, as evidenced by their reported results, which we include herein as our Figure 16.

Sample No.	d_{50}	d_{10}	d_{30}	d_{60}	d_m	σ	$d_{m-\sigma}$	C_c	C_U	n(-)
	mm	mm	mm	mm	mm	mm	mm			
1	0.390	0.29	0.35	0.41	0.39	0.0845	0.31	1.05	1.39	0.344
2	0.390	0.28	0.34	0.41	0.39	0.0852	0.30	1.04	1.48	0.335
3	0.610	0.47	0.55	0.64	0.61	0.1120	0.50	0.99	1.37	0.331
4	0.710	0.53	0.63	0.76	0.72	0.1550	0.57	0.99	1.42	0.340
5	0.840	0.72	0.80	0.86	0.84	0.0921	0.75	1.02	1.19	0.333
6	0.990	0.80	0.91	1.03	0.98	0.1640	0.82	1.01	1.30	0.346
7	1.050	0.89	0.98	1.08	1.05	0.1380	0.91	1.00	1.21	0.348
8	1.360	1.13	1.27	1.41	1.35	0.1890	1.16	1.01	1.25	0.358
9	1.500	1.16	1.34	1.58	1.52	0.2870	1.23	0.98	1.36	0.358
10	2.110	1.72	1.97	2.18	2.07	0.3060	1.76	1.03	1.27	0.357
11	6.340	5.16	5.87	6.55	6.28	0.9380	5.34	1.02	1.27	0.361

Figure 16. *Author's Reported Results.*

As can be seen in Figure 16 herein, for each of the 11 samples studied, which were all reference samples, the authors provide 6 discrete values for particle diameter, d_p, with just 1 corresponding value for external porosity, ε_0 designated as n (-) in the exhibit, and there is no "counterbalancing" value for n_p corresponding to either, (a) each value reported for d_p or, (b) any average value for d_p which would represent the entire distribution of the actual particles packed into any conduit under study. The authors determine the external porosity of the packed conduit by doing mass measurements of the total mass of particles in the packed conduit, in combination with the use of a value for particle density, but this experimental technique is independent of particle diameter assignment. In Figure 17, herein, we have applied Quinn's Law to this data set generating, simultaneously, the values for the Q-modified Ergun coefficients A and B, as well as the values for the Forchheimer coefficients, a and b.

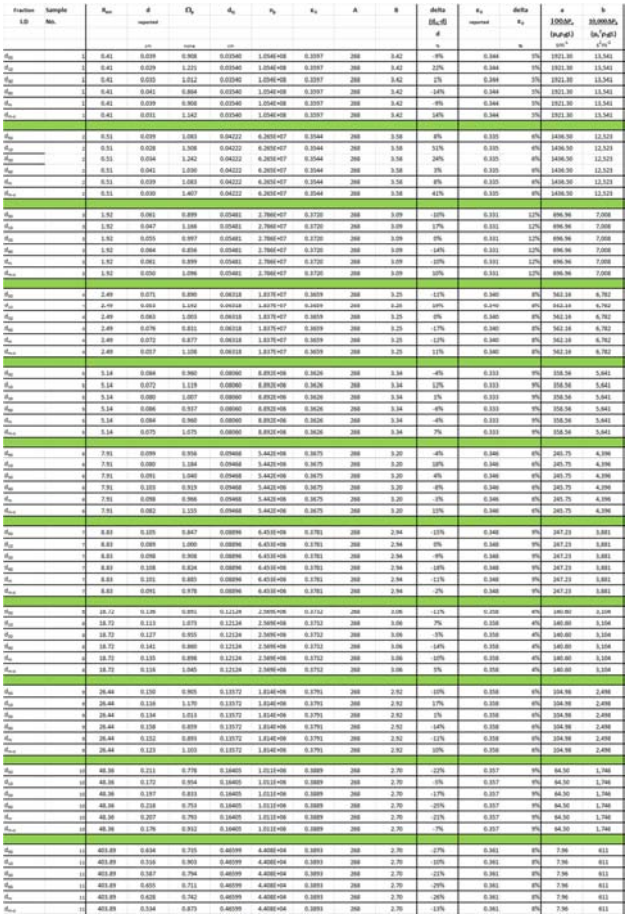

Figure 17. *Elaboration of Author's Results Via Quinn's Law.*

As shown in Figure 17, because, (a) the particles were not spherical and (b) the authors did not report the values for either particle sphericity or the average spherical particle diameter equivalent, we were forced to employ the QFFM model for particle sphericity, Ω_p, to adjust the reported values for particle diameter to values corresponding to the average spherical particle diameter equivalent, which we denote in this paper with the symbol d_Q. This is a necessary characteristic dimension of the particles to employ the Ergun fluid flow model to packed conduit permeability.

Employing the teaching of Quinn's Law, we have deduced a matched set of values for average spherical particle diameter equivalent, d_Q, external porosity, ε_0, and number of particles present, n_p, as well as the corresponding Q-modified Ergun values for A and B, for each of the 11 packed conduits, all of which correlate precisely the reported permeability measurement results. In addition, to demonstrate to the reader the accuracy and precision of the fit obtained between the reported pressure drop values and our calculated values, we have included in the exhibit our back-calculated values for the Forchheimer coefficients, a, and, b. As can be seen from the exhibit, our combination of the values for the two critical parameters, d_Q, and, ε_o, do not correspond to any of the 6 values reported by the authors for particle diameter or their unique value for external porosity. As shown in the exhibit, the discrepancy between the reported values and our values for particle diameter varies between -4 to -26% and 4 to 12% for the values of ε_0. Moreover, we can see that with respect to the Ergun fluid flow model, our calculated value of A for all 11 samples is fixed at 268 approx., but those for the values of B span a range of 2.7 to 3.2 approx. Most importantly, however, our methodology generates the exact same value for d_Q, ε_o and Q-modified values of A and B, independent of whatever particle fraction is chosen. In other words, our methodology determines a unique value for Ω_p for each of the particle sieve fractions reported, which normalizes, in turn, that particle size fraction diameter, and identifies the unique average spherical particle diameter equivalent corresponding to the measured permeability results for the packed conduit containing the entire distribution of particles in that particular conduit.

In Figure 18, we have plotted our results in Figure 17 as friction factor versus modified Reynolds number.

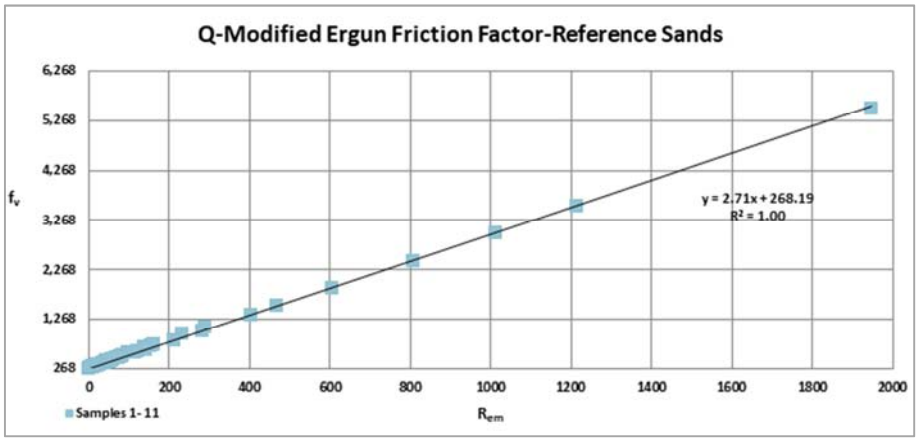

Figure 18. *Q-Modified FF-Reference Sands.*

As can be seen from the Q-modified Ergun viscous-type friction factor plot in Figure 18, to a first approximation, each measured data point for all 11 samples of the reference standards, regardless of the fluid velocity at which the data point was recorded, and regardless of sieve fraction assigned, fall on a straight line of slope B=2.72 and intercept A=268 approximately.

Similarly, as can be seen in Figure 19, herein, for each of the 9 composite samples studied in the paper, we have identified the average spherical particle diameter equivalent using just the d_{50} sieve fraction from the blended reference standards.

Fraction I.D.	Sample No.	R_{em}	d reported	Ω_p	d_Q	n_p	ε_0	A	B	delta $(d_Q-d)/d$	ε_0 reported	delta ε_0	a $100\Delta P_v/(\mu_t \rho g l)$	b $10{,}000\Delta P_k/(\mu_t^2 \rho g l)$
			cm	none	cm					%		%	sm^{-1}	s^2m^{-2}
Composites														
d_{10}	3.1	1.53	0.062	0.915	0.0565	2.592E+07	0.3615	268.19	3.37	-9%	0.334	8%	740.24	8,218.68
d_{10}	4.1	1.61	0.071	0.878	0.0626	1.910E+07	0.3584	268.19	3.45	-12%	0.332	6%	623.59	7,038.64
d_{10}	5.1	3.43	0.084	0.905	0.0761	1.063E+07	0.3593	268.19	3.43	-10%	0.337	7%	418.22	6,351.02
d_{10}	6.1	4.90	0.099	0.800	0.0794	9.263E+06	0.3642	268.19	3.29	-20%	0.330	10%	362.43	5,559.86
d_{10}	6.2	5.63	0.099	0.840	0.0830	8.105E+06	0.3657	268.19	3.25	-16%	0.344	6%	326.48	5,180.79
d_{10}	6.3	7.07	0.099	0.925	0.0915	6.005E+06	0.3696	268.19	3.15	-8%	0.348	6%	256.81	4,380.06
d_{10}	6.4	3.39	0.101	0.763	0.0768	1.036E+07	0.3588	268.19	3.44	-24%	0.332	8%	412.95	6,348.08
d_{10}	7.1	3.98	0.105	0.860	0.0901	6.350E+06	0.3635	268.19	3.31	-14%	0.337	8%	283.75	4,961.07
d_{10}	8.1	10.73	0.136	0.826	0.1126	3.223E+06	0.3703	268.19	3.13	-17%	0.345	7%	168.43	3,518.04

Figure 19. *Composite Samples Elaboration.*

As can be seen from Figure 19 and the plot in Figure 18, all 9 blended samples of the reference particles produced consistent values for the Q- modified values of B.

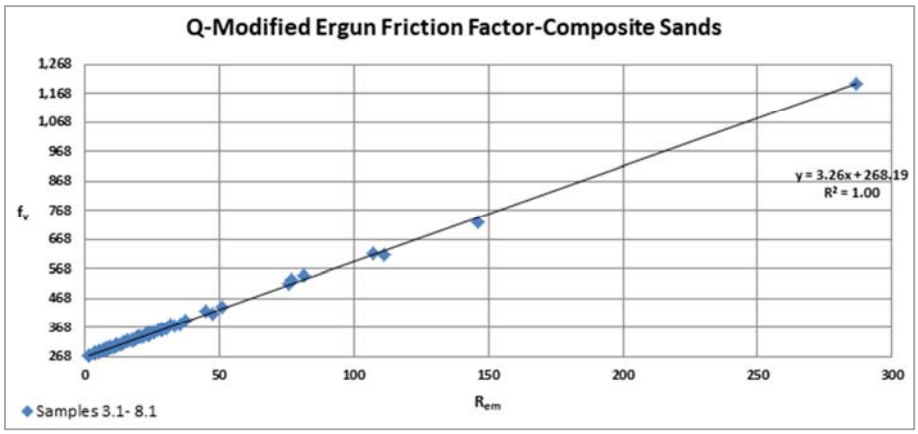

Figure 20. *Q-Modified FF-Composite Sands.*

As demonstrated by the plot in Figure 20, it appears that blending of the reference particles created particle size distributions of varying spherical particle diameter equivalents and slightly elevated values for external porosities than the reference particles packed by themselves and, consequently, slightly elevated values for the Q-modified Ergun coefficient B, whose average value was 3.26, i.e., slightly larger than the average for the reference samples.

Finally, we turn our attention to the more recent study of 2019, in which the authors present additional sample data in that publication. We have analyzed this data set in a similar manner and present our results in Figure 21 and Figure 22.

Fraction I.D.	Sample No.	R_{em}	d reported	Ω_p	d_Q	n_p	ε_0	A	B	delta $(d_Q-d)/d$	ε_0 reported	delta ε_0	a $100\Delta P_x/(\mu_s \rho_f g L)$	b $10{,}000\Delta P_x/(\mu_s^2 \rho_f g L)$
			cm	none	cm					%		%	sm^{-1}	s^2m^{-2}
2019	M.1	4.43	0.045	0.986	0.0444	5.55E+07	0.337	268	4.16	-1%	0.328	3%	1,597.10	16,572
	M.2	4.21	0.054	0.767	0.0414	6.69E+07	0.348	268	3.79	-23%	0.330	5%	1,612.50	14,464
	M.3	5.41	0.077	0.729	0.0561	2.84E+07	0.313	268	5.19	-27%	0.293	7%	1,334.90	21,103
	W.1	6.54	0.148	0.482	0.0714	1.45E+07	0.277	268	7.51	-52%	0.249	11%	1,326.10	36,662
	W.2	12.44	0.950	0.137	0.1298	2.31E+06	0.309	268	5.40	-86%	0.246	26%	263.37	9,958
	S.1	9.48	0.105	0.847	0.0890	6.45E+06	0.378	268	2.94	-15%	0.348	9%	247.23	3,881
	1.1	7.74	0.105	0.705	0.0740	1.14E+07	0.367	268	3.23	-29%	0.346	6%	406.47	5,723
	1.2	7.22	0.105	0.667	0.0700	1.37E+07	0.357	268	3.49	-33%	0.337	6%	505.05	7,155
	1.3	6.14	0.105	0.571	0.0600	2.19E+07	0.353	268	3.62	-43%	0.307	15%	724.65	9,071
	1.4	6.62	0.105	0.644	0.0676	1.60E+07	0.323	268	4.71	-36%	0.285	13%	811.94	14,249
	1.5	5.46	0.105	0.545	0.0573	2.70E+07	0.305	268	5.58	-45%	0.253	21%	1,411.80	24,222
	S.2	14.49	0.150	0.905	0.1357	1.81E+06	0.379	268	2.92	-10%	0.358	6%	104.98	2,498
	2.1	12.00	0.150	0.756	0.1134	3.14E+06	0.374	268	3.05	-24%	0.358	4%	159.56	3,282
	2.2	9.35	0.150	0.607	0.0910	6.24E+06	0.355	268	3.55	-39%	0.334	6%	306.29	5,726
	2.3	7.60	0.150	0.514	0.0770	1.07E+07	0.329	268	4.48	-49%	0.307	7%	584.96	11,219
	2.4	6.82	0.150	0.470	0.0705	1.43E+07	0.315	268	5.11	-53%	0.265	19%	829.69	16,280
	2.5	5.55	0.150	0.396	0.0594	2.47E+07	0.291	268	6.43	-60%	0.242	20%	1,573.50	31,612
	S.3	50.56	0.634	0.735	0.4660	4.41E+04	0.389	268	2.70	-27%	0.361	8%	7.96	611
	3.1	23.58	0.634	0.350	0.2216	4.18E+05	0.377	268	2.96	-65%	0.324	16%	40.16	1,577
	3.2	14.57	0.634	0.234	0.1482	1.51E+06	0.326	268	4.61	-77%	0.252	29%	163.84	6,187
	3.3	5.25	0.634	0.058	0.0370	6.71E+07	0.533	268	1.05	-94%	0.227	135%	287.55	894

Figure 21. *Elaboration of 2019 Reported Results.*

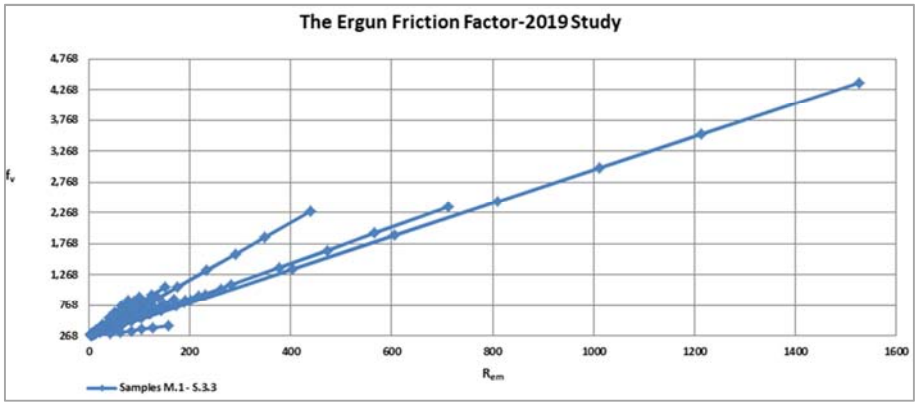

Figure 22. *Q-Modified FF -2019 Study.*

As can be seen from Figure 21, herein, it is obvious that the particle shapes of the reference materials used for the blending process in this study, were more irregular that in the 2017 study. This resulted in a broader range of external porosity values for the packed conduits, which, in turn, generated a broader range of values for the Q-modified Ergun B values resulting in a series of lines with different slopes for each conduit in the friction factor plot of Figure 22 for these samples.

5.2. Discussion

In the 2017 paper there are two sets of modified Ergun coefficients, A and B, reported which are purported to correlate the measured data and, accordingly, predict the coefficients a and b accurately. One set is reported in the abstract, A=139.1, B=2.2 (d_m), and one in the conclusion, A=183.8, B=2.53 (d_{30}). Likewise, in the abstract of the 2019 paper, there is an additional reference for that paper, A=63.1 and B=1.72 (d_{10}).

We have applied these values as reported in the papers and captured our results in Figure 23 and Figure 24.

Fraction I.D.	Sample No.	R_{em}	d reported	Ω_p	d_Ω	n_p	ε_0	A	B	delta $\frac{(d_\Omega - d)}{d}$	ε_0 reported	delta ε_0	a $\frac{100\Delta P_v}{(\mu_s \rho g L)}$	b $\frac{10{,}000\Delta P_k}{(\mu_s^2 \rho g L)}$
			cm	none	cm					%		%	sm^{-1}	s^2m^{-2}
d_{30}	1	0.39	0.035	1.000	0.03500	1.118E+08	0.3440	184	2.53	0%	0.344	0%	1616.86	11,874
$d_{m-\sigma}$	1	0.35	0.031	1.000	0.03100	1.608E+08	0.3440	139	2.20	0%	0.344	0%	1559.79	11,658
d_{10}	M.1	1.97	0.020	1.000	0.02000	6.135E+08	0.3280	63	1.72	0%	0.328	0%	2057.87	16,695

Figure 23. *Author's Reported Values of A and B.*

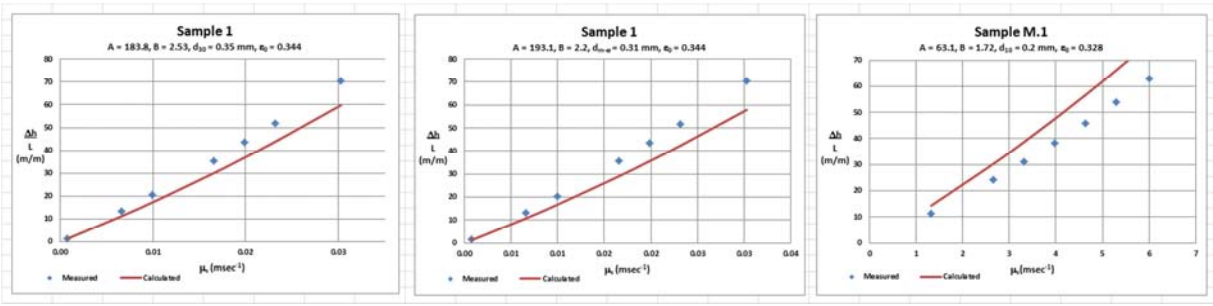

Figure 24. *Author's Reported Correlations.*

As can be seen from Figure 23, none of the 3 sets of modified Ergun coefficients generate accurate values for the Forchheimer coefficients, a, and b. Similarly, Figure 24 demonstrates that the correlation between measured and calculated results is unacceptable, for all three examples.

For comparison purposes, we have included in Figure 25 the correlation provided by Quinn's Law for both samples 1 and M. 1.

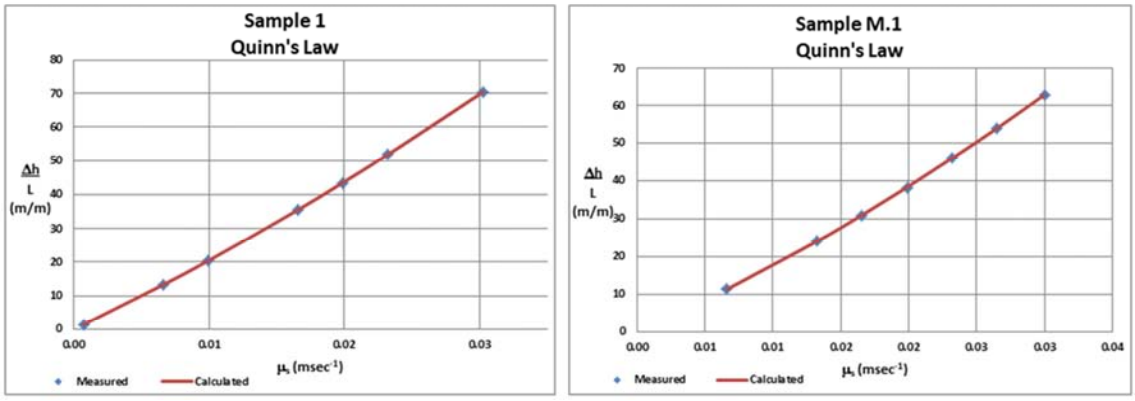

Figure 25. *Quinn's Law Correlations.*

As can be observed from our exhibits herein, the accuracy and precision of the specified values for the Forchheimer coefficients a and b, in this worked example, requires an experimental protocol, whose degree of accuracy and precision regarding the measurement of particle diameter, d_p, and external porosity, ε_0, is much greater than that employed by the authors in this example. Of course, we must state that in our analysis, we have assumed that the measurements underlying the values of the specified Forchheimer coefficients, a, and b, were both accurate and precise. Otherwise, all bets are off regarding our analysis conclusions.

On the other hand, the experimental protocol disclosed in

this paper underlying Quinn's Law, does not suffer from the same lack of accuracy/precision. Accordingly, Quinn's Law, having been validated by this extremely accurate and precise experimental protocol, can now be used to back-calculate the unique combination of values for d_p, ε_0 and n_p, for any data set, whose values for the Forchheimer coefficients a and b are provided as a given together with fluid properties, anywhere across the entire spectrum of the fluid flow regime.

6. Conclusions

In this paper we have demonstrated that the recent publication of Quinn's Law has enabled us to clearly demonstrate the shortcomings of the Ergun equation in a manner which is both comprehensive and easy to understand. Moreover, it has allowed us to reinvent the Ergun equation after the teaching of Quinn's Law, and produce a modified version which we call herein the Q-Modified Ergun equation.

The viscous type friction factor derived from the Q-Modified Ergun equation has the general format of $f_v=A + BR_{em}$, where the value of $A=256\pi/3$ (268 approx.), and the value of $B=1/(2\pi\varepsilon_0^3)$. Accordingly, it is now clear that the external porosity parameter, ε_0, plays an extraordinarily dominant role in the permeability of packed conduits, particularly when the fluid flow profile is dominated by the kinetic term of the equation, i.e., the so-called turbulent regime.

The value of A in the Q-Modified Ergun equation is significantly larger than the value of 150 assigned by Ergun in his 1952 publication. Thus, the conventional Ergun equation always understates the pressure gradient when the fluid flow profile is dominated by the viscous term in the equation, i.e., the so-called laminar region.

Importantly, we have demonstrated herein an experimental protocol which is unique in the literature for packed conduits. It is an empirical technique that is self-calibrating to the extent that it;

1. Defines the length of the packed conduit under study in terms of the average spherical particle diameter equivalent assigned.
2. Establishes the experimental technique of defining the external porosity of the packed conduit in terms of the number of actual whole particles placed within the conduit, in combination with the conduit length expressed as a function of the spherical particle diameter equivalent.
3. Compares the permeability measurements of an empty and packed conduit, demonstrating a cross calibration methodology, which removes any ambiguity due to the measurement of particle diameter or external porosity in a packed conduit.

Finally, due to the specialized nature of our experimental methodology disclosed herein, this paper eliminates any issues related to the size distribution of particles. In other words, this paper discloses an experimental technique which is self-calibrating for particle size distribution and which renders obsolete the fundamentally erroneous practice of adjusting the value of A and B in the Ergun model, to accommodate this so-called phenomenon. Accordingly, we have emphatically demonstrated herein that the value of A is always 268 (approximately) and is independent of particle size, particle size distribution and fluid flow profile.

Conflict of Interest

The authors declare that they have no competing interests.

References

[1] Quinn, H. M. Quinn's Law of Fluid Dynamics Pressure-driven Fluid Flow Through Closed Conduits, *Fluid Mechanics*. Vol. 5, No. 2, 2019, pp. 39-71. doi: 10.11648/j.fm.20190502.12.

[2] Ergun, S. and Orning, A. A., Fluid Flow through Randomly Packed Columns and Fluidized Beds, Ind. Eng. Chem. vol. 41, pp. 1179, 1949.

[3] Ergun, S., Determination of Particle Density of Crushed Porous Solids, Anal. Chem. vol. 23, 1951.

[4] Ergun, S., Fluid Flow Through Packed Columns, Chem. Eng. Progr. vol. 48, pp. 89-94, 1952.

[5] Farkas, T., Zhong, G., Guiochon G.,, Validity of Darcy's Law at Low Flow Rates in Liquid Chromatography Journal of Chromatography A, 849, (1999) 35-43.

[6] Quinn, H. M., Quinn's Law of Fluid Dynamics: Supplement #1 Nikuradze's Inflection Profile Revisited, *Fluid Mechanics*. Vol. 6, No. 1, 2020, pp. 1-14. doi: 10.11648/j.fm.20200601.11.

[7] Quinn, H. M., Reconciliation of Conventional Wisdom with Reality. A Misconstrued Constant Used as a Tool to Manipulate Paying Customers. Lambert Academic Publishing (2019).

[8] Poiseuille, J. L. M., Memoires des Savants Etrangers, Vol. IX pp. 435-544, (1846); BRILLOUIN, M. (1930) Jean Leonard Marie Poiseuille. Journal of Rheology, 1, 345.

[9] Van Lopik, J. H., Snoeijers, R., Van Dooren, T. C. G., Raoof, A., Schotting, R. J., The Effect of Grain Size Distribution on Nonlinear Flow Behavior in Sandy Porous Media, Transp Porous Med (2017) 120: 37-66. DOT. 10.1007/s11242-017-0903-3.

[10] Van Lopik, J. H., Zazai, L., Hartog, N., Schotting, R. J., Nonlinear Flow behavior in Packed Beds of Natural and Variably Graded Granular Materials, Transp Porous Med, https://dci.org/10.1007/s11242-019-01373-0 (2019).